

1           **SWAT-Tb with improved LAI representation in the**  
2           **tropics highlights the role of forests in watershed**  
3           **regulation**

4           **Santiago Valencia<sup>1</sup>, Juan F. Salazar<sup>1</sup>, Juan Camilo Villegas<sup>2</sup>, Natalia Hoyos<sup>3</sup>,**  
5           **Mateo Duque-Villegas<sup>1,4,5</sup>**

6           <sup>1</sup>GIGA, Escuela Ambiental, Facultad de Ingeniería, Universidad de Antioquia, Medellín, Colombia  
7           <sup>2</sup>Grupo de investigación en Ecología Aplicada, Escuela Ambiental, Facultad de Ingeniería, Universidad de

8           Antioquia, Medellín, Colombia

9           <sup>3</sup>Department of History and Social Sciences, Universidad del Norte, Barranquilla 080001, Colombia

10           <sup>4</sup>Max Planck Institute for Meteorology, Hamburg, Germany

11           <sup>5</sup>International Max Planck Research School on Earth System Modelling, Hamburg, Germany

12           **Key Points:**

- 13           • New SWAT (Soil and Water Assessment Tool) model variant captures bimodal  
14           tropical vegetation dynamics
- 15           • Seasonality of streamflow anomalies is switched due to forest-to-pasture conver-  
16           sion
- 17           • Deforestation exacerbates low flows during dry season
- 18           • Standard SWAT leads to misleading conclusion about deforestation impacts

19 **Abstract**

20 Projecting the potential impacts of LULC (Land Use/Land Cover) change on watershed  
 21 hydrological response is critical for water management decisions in a changing environment.  
 22 An improved representation of vegetation dynamics is needed to improve the capability of  
 23 several hydrological models to produce reliable projections of these impacts. Here we in-  
 24 troduce a modification in the plant growth module of SWAT (Soil Water Assessment Tool)  
 25 to improve the representation of the bimodal seasonality of LAI (Leaf Area Index), which  
 26 is particularly important for tropical watersheds with bimodal precipitation regimes. The  
 27 new SWAT-Tb variant that we propose here reproduces not only observed streamflow, but  
 28 also the bimodal seasonal pattern of LAI in a tropical mountain watershed of the Andes. In  
 29 contrast, standard SWAT is inherently unable to reproduce this bimodality, although it can  
 30 be calibrated to reproduce streamflow. Differences between models in the representation  
 31 of LAI seasonality can lead to significantly different results about LULC change impacts  
 32 on streamflow. SWAT-Tb results show that deforestation impacts on streamflow are more  
 33 pronounced for seasonal than for annual streamflow, and indicate that forests can play a  
 34 crucial role in enhancing water availability during dry seasons. The seasonality of streamflow  
 35 anomalies is switched due to forest-to-pasture conversion, implying that while forest ex-  
 36 pansion increases water availability in dry seasons, forest conversion into pasture decreases it.  
 37 Due to its poor representation of LAI seasonality, standard SWAT largely underestimates  
 38 this role of forest, which can be misleading for decision making about water security and  
 39 forest conservation.

40 **1 Introduction**

41 Changes in Land Use/Land Cover (LULC henceforth) lead to some of the most concerning  
 42 anthropogenic alterations of hydrological processes and concomitant environmental and  
 43 social phenomena (Foley et al., 2005; M. Zhang et al., 2017). In a watershed, the trans-  
 44 formation of LULC affects multiple aspects and components of the surface water balance,  
 45 including soil permeability (Benavides et al., 2018), evapotranspiration (Ponette-González  
 46 et al., 2014), surface runoff (Roa-García et al., 2011), infiltration (Marín et al., 2019), base  
 47 flow, water yield (Ochoa-Tocachi et al., 2016), energy partitioning (Mercado-Bettín et al.,  
 48 2019), and, ultimately, the watershed response via streamflow (Muñoz-Villers & McDonnell,  
 49 2013; Ramírez et al., 2017) and regulation capacity (e.g. the amplitude of the streamflow  
 50 regime) (Ochoa-Tocachi et al., 2016; Peña-Arancibia et al., 2019; J. F. Salazar et al., 2018).  
 51 Projecting the potential impacts of LULC change on watershed response and regulation is  
 52 critical for water management decisions in a changing environment (Montanari et al., 2013;  
 53 J. F. Salazar et al., 2018).

54 Deforestation is one of the most relevant forms of LULC change, especially in regions like  
 55 tropical South America with historically high deforestation rates that may be exacerbated by  
 56 climate change and complex social issues (Zemp et al., 2017; A. Salazar et al., 2018; Duque-  
 57 Villegas et al., 2019). This is particularly problematic in the tropical Andes, where water and  
 58 related energy security rely largely on streamflow from mountain watersheds (Viviroli et al.,  
 59 2007; Sáenz et al., 2014; Angarita et al., 2018; Immerzeel et al., 2020). Major LULC trends  
 60 in this region include the transformation of Andean forest and paramo vegetation to pastures  
 61 for cattle raising (García-Leoz et al., 2017), agricultural systems (Clerici et al., 2019), and  
 62 forest plantations (Bonnesoeur et al., 2019). Field observations show that forest conversion  
 63 into pasture or crops is associated with changes in the water balance components and related  
 64 surface properties such as soil permeability, surface runoff, and infiltration (Ramírez et al.,  
 65 2017; Marín et al., 2019; Suescún et al., 2017). Therefore, understanding the potential  
 66 impacts of forest loss on streamflow is needed for the assessment of threats to sustainability,  
 67 especially in mountain watersheds that are becoming increasingly critical for water security  
 68 in lowland populations (Immerzeel et al., 2020; Viviroli et al., 2020).

The effects of LULC change on watershed response are largely assessed through hydrological models (e.g. M. Zhang et al., 2017; Dos Santos et al., 2018; Peña-Arancibia et al., 2019). Hydrological models are generally able to reproduce observed streamflow (Krysanova et al., 2017). This is a result of, first, models being built upon physical principles, the main of which is mass (water) conservation; and second, of models having numerous parameters that can be tuned to reproduce observations (i.e. model calibration). However, the capability of making reliable projections (e.g. for LULC scenarios) depends on the potential of these models to reproduce the system's behavior for the right reasons (Kirchner, 2006). When the performance of hydrological models is largely, or exclusively, evaluated by comparing simulated and observed streamflow (e.g. Setegn et al., 2010; Villamizar et al., 2019), there is a danger of ignoring unrealistic representations of other important water balance components and related processes.

The Soil and Water Assessment Tool (SWAT) is among the most widely used hydrological models for investigating LULC change impacts on watershed response (Marin et al., 2020; Tan et al., 2020). One of the most critical model components for this task is the vegetation dynamics module (Strauch & Volk, 2013; Alemayehu et al., 2017), since it directly affects the surface water and energy balances (Bonan, 2008). This module includes a plant growth scheme that was originally developed for temperate regions (Neitsch et al., 2011) and, therefore, is not necessarily adequate for tropical regions (Strauch & Volk, 2013; Alemayehu et al., 2017; Hoyos et al., 2019; H. Zhang et al., 2020). This limitation has been partially addressed by using the Leaf Area Index (LAI) to represent vegetation dynamics (Strauch & Volk, 2013; Alemayehu et al., 2017; Ma et al., 2019; Rajib et al., 2020). For instance, Alemayehu et al. (2017) developed a SWAT variant (named SWAT-T) that improves the representation of LAI seasonality in tropical ecosystems, yet still fails to reproduce the bimodal seasonality of LAI that is typical of many of them (Ye et al., 2021) and that is related to the seasonal migration of the ITCZ (Urrea et al., 2019; Knoben et al., 2019). An improved representation of vegetation dynamics is needed to improve the potential of SWAT to produce reliable projections of LULC change impacts (Marin et al., 2020).

The goals of the present study were, first, to improve the representation of tropical vegetation dynamics in SWAT, and then to use the improved model for studying the potential impacts of LULC change on the response of a tropical watershed. More specifically, here we introduce a modification in the plant growth module of SWAT to improve the representation of LAI seasonality, which leads to a new variant that we refer to as SWAT-Tb. Then we compare the performance of SWAT-Tb with other SWAT variants (i.e. standard or default SWAT (Revision 627) and SWAT-T), and show that, in contrast to these other variants, SWAT-Tb produces a realistic representation of not only streamflow but also LAI. Finally, we use SWAT-Tb to study the potential effects of LULC change on streamflow, particularly the expansion of either forest or pasture cover, in a tropical mountain watershed; and show that using the standard SWAT can lead to misleading conclusions.

## 2 Revision of SWAT Model

The new variant of SWAT, namely SWAT-Tb, introduces a bimodal representation of vegetation dynamics into the SWAT-T model of Alemayehu et al. (2017). SWAT-Tb accounts for the bimodal seasonality of LAI that is typical of many watersheds in tropical (Hoyos et al., 2019; Knoben et al., 2019) and non-tropical (Alhamad et al., 2007; Yang et al., 2019) regions. In the following sections, we provide background on the SWAT model and explain the changes in the new variant.

### 2.1 Model Description and Limitations

SWAT is a public domain, watershed-scale, process-based, hydrological model (Arnold et al., 1998; Neitsch et al., 2011) that can simulate the response of watersheds (e.g. streamflow) to a variety of forcings, including both climate and LULC change (Gassman et al., 2014; Tan

et al., 2020). It is a semi-distributed model wherein a watershed is divided into sub-basins that are further divided into Hydrologic Response Units (HRUs), which are characterized by uniform soil, slope, LULC, and management attributes. Hydrological processes simulated by SWAT include evapotranspiration, surface runoff, percolation, lateral flow, groundwater flow, transmission losses, and ponds (Arnold et al., 2012). The model also includes parameterizations for processes such as plant growth, erosion, nutrients cycling, and pesticides degradation (Neitsch et al., 2011).

The most common formulation for vegetation dynamics in SWAT uses a plant growth module that simulates leaf area development, light interception, and conversion of intercepted light into biomass (Neitsch et al., 2011). This module is based on the Environmental Policy Impact Climate (EPIC) model (Williams et al., 1989) that was developed for temperate regions and is not suitable for all tropical regions (Strauch & Volk, 2013; Alemayehu et al., 2017). A key reason for this is that the EPIC-based module assumes that plant growth, including leaf area development, is mainly controlled by variations in temperature and daylength, which is especially relevant for temperate environments (Mwangi et al., 2016). For instance, this module assumes that plant growth is reduced as daylength approaches that of the shortest day of the year (winter solstice) due to dormancy (Arnold et al., 1998). However, tropical vegetation dynamics can be much less influenced by temperature and daylength-driven dormancy (Ma et al., 2019), and instead much more controlled by precipitation through soil moisture (X. Zhang et al., 2006). Indeed, in our study watershed, seasonal LAI is more related to precipitation than to temperature (see Section 4.1). This model limitation and its implications for water balance have been highlighted in several studies (Wagner et al., 2011; Strauch & Volk, 2013; Alemayehu et al., 2017; Hoyos et al., 2019; Ma et al., 2019; Rajib et al., 2020; H. Zhang et al., 2020; Marin et al., 2020).

Recognizing this limitation, previous studies have introduced novel representations of vegetation dynamics into SWAT, which have produced satisfactory results for regions like Central Brazil (Strauch & Volk, 2013), Kenya and Tanzania (Alemayehu et al., 2017), southeast China (Ma et al., 2019), north central United States (Rajib et al., 2020), and northern Australia (H. Zhang et al., 2020). For instance, Alemayehu et al. (2017) successfully implemented their new SWAT-T variant in a tropical watershed in Kenya and Tanzania after having modified the plant growth module. Many tropical watersheds, however, do not conform to the unimodal cycle as prescribed in SWAT-T. In fact, Hoyos et al. (2019) showed that although SWAT-T successfully reproduces streamflow in a watershed of the tropical Andes and improves the representation of LAI dynamics as compared to SWAT, it nevertheless fails in reproducing the observed bimodal seasonality of LAI.

## 2.2 Changes in Plant Growth Module in SWAT-Tb

We built upon SWAT-T's vegetation module to develop SWAT-Tb. This enhanced module has the capability of representing a bimodal LAI annual cycle. SWAT-T uses changes in the Soil Moisture Index (SMI, computed as the ratio between 5-day aggregate precipitation (P) and reference evapotranspiration (ET)) as a proxy for the dry to wet season transition in the tropics, which then triggers a unimodal vegetation growth cycle (Alemayehu et al., 2017). Unlike SWAT-T, SWAT-Tb uses precipitation as a proxy for seasonal variations in LAI. This relation is based also on the assumption that the onset of the wet season triggers plant growth (Liang et al., 2020), and agrees with observations of the annual cycles of precipitation and LAI in the study watershed (see Section 4.1). Using precipitation (as in SWAT-Tb) instead of SMI (as in SWAT-T) is also consistent with the fact that tropical environments are not always water-limited (Gotsch et al., 2016), therefore there is not always a direct relation between plant growth and soil moisture (Alemayehu et al., 2017). In the energy-limited environments that are common in the tropical Andes, precipitation is arguably a better proxy of vegetation dynamics because it relates to both water and energy (e.g. peak LAI comes after peak precipitation as shown in Section 4.1). Seasonal precipitation in the tropical Andes is strongly controlled by the latitudinal migration of the ITCZ (Espinoza et

**Table 1.** Description of data used in this study.

Data	Description	Source
DEM	Elevation data at a resolution of 1 arc-second (30 meters).	Jarvis et al. (2008)
Land cover	Land cover map for the Grande and Chico rivers watersheds for the year 2015, scale 1:100,000.	CORANTIOQUIA and UNAL (2015)
Soil	Soil map for the the Grande and Chico rivers watersheds, scale 1:50,000.	Machado et al. (2019)
Hydrometeorological	Precipitation, minimum and maximum temperature, relative humidity, evapotranspiration, and streamflow for the period 1990–2016.	EPM <sup>1</sup> and IDEAM <sup>2</sup>
LAI	MCD15A2Hv006 MODIS-LAI product for the period 2003–2016 with a spatial resolution of 0.5 km. Values are 8-days-composites.	Myneni et al. (2015)

<sup>1</sup>EPM: Public Utilities Company of Medellín, <sup>2</sup>IDEAM: Colombian Institute of Hydrology, Meteorology and Environmental Studies.

al., 2020), which affects the surface energy balance, and therefore other vegetation-related variables such as photosynthetic rate, net productivity, and transpiration (Aparecido et al., 2018). The SWAT-Tb executable and the associated changes with file examples (\*.sub, \*.mgt and plant.dat) can be found in Supplementary Material S1.

### 3 Materials and Methods

#### 3.1 Study Area

This study focuses on the Chico River (CR) watershed in the tropical Andes of Colombia (Figure 1). The CR watershed is a tributary of the Grande River (GR) watershed, which is strategic for water supply to local rural communities and more than 4 million people living in the Metropolitan Area around Medellín, as well as for hydropower generation (the CR flows into a reservoir, Figure 1d), agriculture, and dairy industry. The CR watershed covers a drainage area of 169 km<sup>2</sup> with altitudes ranging between 2400 and 3260 m.a.s.l. (Figure 1e). Mean annual precipitation is 1820 mm, and mean monthly temperature varies between 12°C and 16°C with an average of 14°C. Precipitation seasonality is characterized by a bimodal regime with two wet seasons: March-April-May (MAM) and September-October-November (SON), and two dry seasons: December-January-February (DJF) and June-July-August (JJA) (Poveda, 2004; García-Leoz et al., 2017). Land use in the watershed is dominated by pastures (54.17% of the area), followed by native forest (29.30%), shrubs (11.42%), and paramo vegetation (4.89%) (Figure 1e). A considerable fraction of native vegetation (e.g. native forest, shrubs, and paramo vegetation) has been converted into agro-pastoral uses in the watershed (Berrouet et al., 2020). The dominant soil type is Andic Dystrudepts, which makes up 62% of the watershed (Figure 1g).

#### 3.2 Input Datasets and Model Parameters

A summarized description of the data used in this study and their sources are presented in Table 1. Elevation data were used for the definition of sub-basins and HRUs. Based on previous studies for tropical Andean regions, the LULC map was reclassified to match the SWAT land use types (Supplementary Table S1; (Tapasco et al., 2015; Hoyos et al., 2019; Villamizar et al., 2019)), and the soil map was parameterized (Machado et al., 2019; Uribe et al., 2018, 2020). Processing of the above data yielded 7 sub-basins and 649 HRUs using the SWAT2012 extension (version 1.9) within QGIS 2.6.1 (Dile et al., 2019) software.

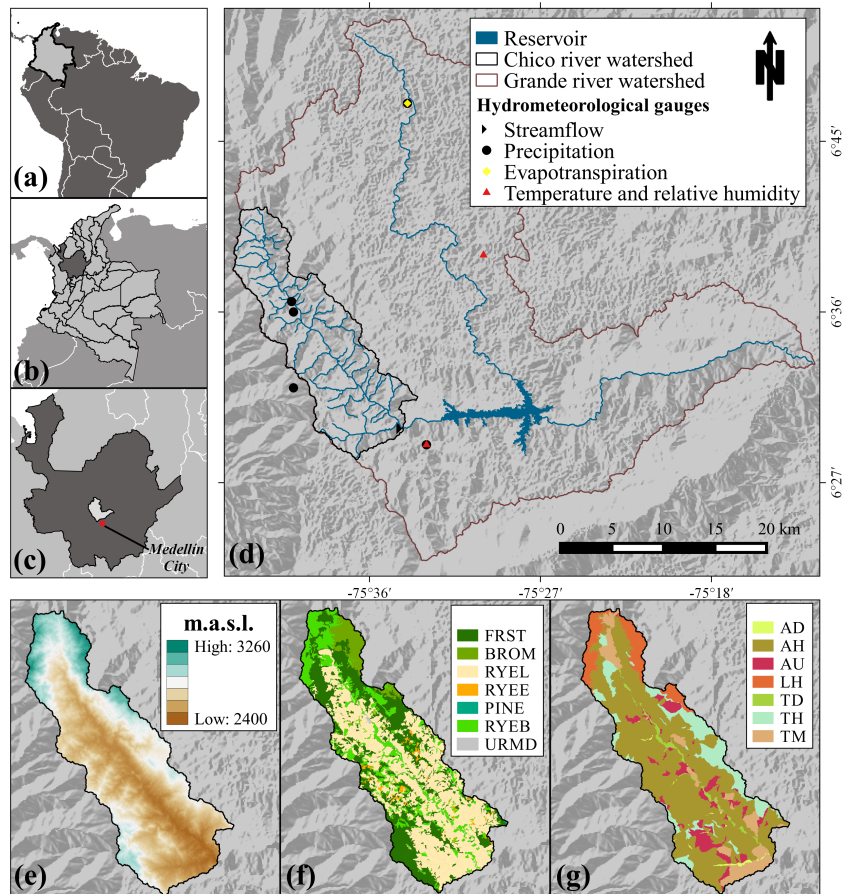


**Figure 1.** (a-c) General location of the study area (South America, Colombia, and Antioquia, respectively). (d) Grande (“big”) and Chico (“small”) rivers watersheds including hydrometeorological gauges. (e) Digital Elevation Model (DEM), (f) land cover for the year 2015, and (g) soil types. Land cover and soil types codes are: RYEL: pasture, FRST: native Andean forest, RYEB: shrubs, BROM: paramo vegetation, RYEE: pasture with secondary growth, PINE: planted forest, URMD: urban, AD: Andic Dystrudepts, AH: Andic Humudepts, AU: Andic Udifluvents, LH: Lithic Hapludand, TD: Typic Dystrudepts, TH: Typic Hapludands, and TM: typic melanudands.

Daily hydrometeorological data (precipitation, maximum and minimum temperature, relative humidity, evapotranspiration, and streamflow) from the available gauges (Figure 1d) were provided by the Colombian Institute of Hydrology, Meteorology and Environmental Studies (IDEAM in Spanish) and the Public Utilities Company of Medellín (EPM in Spanish). We used the Priestley-Taylor equation to calculate evapotranspiration as wind data were not available from ground-based gauges, and global datasets (reanalyses) have a limited capacity to represent wind over the complex terrain of the Andes (Posada-Marín et al., 2019). The SWAT's internal WGENX weather generator (Neitsch et al., 2011) was used to estimate daily solar radiation. Observed 8-day composites of LAI were obtained from the MCD15A2H-MODIS product (Myneni et al., 2015) for the 2003–2016 period at 0.5 km spatial resolution. Further details on LAI data processing are given in Section S2 of the Supplementary Material.

### 3.3 Model Calibration, Validation and Uncertainty Estimation

The SWAT-Tb model is calibrated to simulate, first, monthly LAI, and then monthly streamflow using both manual and automatized techniques. Parameters are initially selected based on a literature review (Arnold et al., 2012; Strauch & Volk, 2013; Abbaspour et al., 2015; Alemayehu et al., 2017; H. Zhang et al., 2020) that includes previous studies for Andean watersheds (Tapasco et al., 2015; Hasan & Wyseure, 2018; Hoyos et al., 2019; Villamizar et al., 2019) (Supplementary Table S3). In order to obtain comparable results, SWAT-T is also calibrated for LAI whereas SWAT is only calibrated for streamflow. Streamflow and LAI calibration was conducted for 2003–2016, while validation was performed for 1993–2002. Three years are added at the beginning of each simulation as a spin-up period to mitigate the influence of uncertain initial conditions, especially for soil moisture. Sensitivity and uncertainty analyses, as well as automatized procedures for calibration and validation are carried out in SWAT-CUP 2019 (version 5.2.1; Abbaspour, 2013) using the Sequential Uncertainty Fitting (SUFI-2) algorithm (Abbaspour et al., 2004).

Calibration of LAI is performed for SWAT-Tb and SWAT-T through manual adjustment of parameters (Supplementary Table S2) while considering land cover types separately. The Breaks for Additive Seasonal and Trend (BFAST) method (Verbesselt et al., 2010) was implemented to exclude noise from the LAI time series. The Pearson correlation coefficient ( $r$ ), the percent bias (PBIAS), and the Kling–Gupta efficiency (KGE; Gupta et al., 2009) are used to evaluate the agreement between simulated and observed LAI values. Since we want to assess the effect of an inaccurate representation of vegetation dynamics, SWAT is not calibrated for LAI, which is not an unusual practice (e.g. Villamizar et al., 2019; Adhikari et al., 2020). Streamflow calibration is focused on the dominant land cover types—pasture (RYEL) and native Andean forest (FRST) that account for approximately 80% of the watershed (Figure 1f)—and on the upper soil layers that are most directly affected by vegetation change (Tobón et al., 2010; Marín et al., 2019). Parameters for the dominant land cover types are calibrated independently, whereas parameters for all other land cover types are grouped in order to reduce computational cost.

Sensitive parameters are identified with a sensitivity analysis based on 500 simulations. This analysis starts with 33 parameters selected based on previous studies and literature review (Supplementary Table S3), and yields 18 of them as the most sensitive ( $p$ -value  $\leq 0.05$ , Supplementary Table S4). We also define an acceptable range of variability for each sensitive parameter. Subsequently, we calibrate monthly streamflow with SUFI-2 using 1000 simulations per iteration (Latin hypercube sampling) for the selected parameter ranges. The calibration goal is to obtain acceptable values for uncertainty statistics ( $p$ -value and  $r$ -value) and the performance criteria proposed by Moriasi et al. (2007), which include Nash-Sutcliffe Efficiency (NSE) as the objective function and other complementary statistics: percent bias (PBIAS), determination coefficient, and RMSE-observations standard deviation ratio (RSR). We also seek to obtain a reasonable representation of water balance components by considering the following metrics: fraction of total runoff as baseflow, ratio between

total evapotranspiration and total precipitation, and ratio between surface runoff and total streamflow. Model outputs for these metrics are compared with observation-based estimates for Andean watersheds (Jaramillo-Robledo, 2003; García-Leoz et al., 2017; Suescún et al., 2017; Bonnesoeur et al., 2019; Marín et al., 2019) (Supplementary Table S4).

### 257 3.4 LULC Scenarios

258 A control (CTL) scenario (i.e. LULC distribution for 2015 (CORANTIOQUIA &  
 259 UNAL, 2015), Figure 1f) and two extreme LULC scenarios are simulated: full watershed  
 260 forest loss (100% pasture, PAS) and forest cover (100% forest, FOR). These are not real-  
 261 istic but “baseline”-type scenarios that are used to study the range of potential changes  
 262 in streamflow due to forest change in the watershed (e.g. Alvarenga et al., 2016; Tian et  
 263 al., 2017; Li et al., 2019; Peña-Arancibia et al., 2019). These scenarios not only represent  
 264 changes in the cover (e.g. LAI) but also in some soil properties based on parameteriza-  
 265 tion of land cover types, to obtain a more realistic assessment of forest loss and intensive  
 266 pasture management impacts on water balance (Tobón et al., 2010; Marín et al., 2019; Peña-  
 267 Arancibia et al., 2019). Each scenario is simulated for the period 1993–2016 (plus a spin-up  
 268 period of three years) using the best-fit parameter values from the calibration along with  
 269 1000 random combinations within the acceptable ranges. These simulations are performed  
 270 using the SUFI-2 algorithm (Abbaspour et al., 2004) and their output is used to assess the  
 271 effects of parameter variability and uncertainty on the results. Differences between scenarios  
 272 are analyzed using the non-parametric Wilcoxon rank-sum and signed-rank tests (Bauer,  
 273 1972). Since everything else is equal, these differences are entirely attributable to LULC  
 274 change.

### 275 3.5 Comparison of SWAT variants

276 Three variants of the SWAT model that differ in their plant growth module are used:  
 277 SWAT (default version, Arnold et al., 2012), SWAT-T (Alemayehu et al., 2017), and SWAT-  
 278 Tb (present study). These variants are compared to evaluate their performance in repro-  
 279 ducing the observed dynamics of plant growth, specifically LAI (see Section 4.1). As a  
 280 proof-of-concept, we also compare SWAT calibrated for streamflow with SWAT-Tb cali-  
 281 brated for both LAI and streamflow.

## 282 4 Results

### 283 4.1 LAI Calibration

284 The observed seasonality of precipitation and LAI for all vegetation types in the wa-  
 285 tershed exhibits a marked bimodal regime (Figure 2). There are two wet seasons in MAM  
 286 and SON, and two “dry” (less rainy) seasons in DJF and JJA. The SMI follows this same  
 287 pattern. Relative to precipitation and SMI, LAI exhibits a pattern that can be described  
 288 as mirrored to precipitation with lower values around the wet seasons and higher values in  
 289 the dry seasons, which indicates energy-limited ecosystems. This suggests that during the  
 290 dry seasons plant growth is not as limited by reduced precipitation and moisture (SMI is  
 291 greater than 1 in all months but January) as it is enhanced by increased radiation resulting  
 292 from less cloud cover (Aparecido et al., 2018). These results confirm the role of precipita-  
 293 tion (and cloudiness) in controlling vegetation seasonality, which according to our results  
 294 and previous observations appears to be greater than that exerted by temperature. This  
 295 contrasts the assumptions made in the EPIC model about the dominant role of temperature  
 296 in plant growth (Williams et al., 1989; Arnold et al., 2012).

297 Comparison between observed and simulated LAI using SWAT, SWAT-T, and SWAT-  
 298 Tb for the dominant LULC types shows that SWAT fails to represent LAI seasonality, as  
 299 evinced by high biases ( $53\% < |\text{PBIAS}| < 90\%$ ) and negative or low correlations ( $-0.51 <$   
 300  $r < 0.13$ ). Results for other LULC types are shown in Supplementary Figure S1. A default

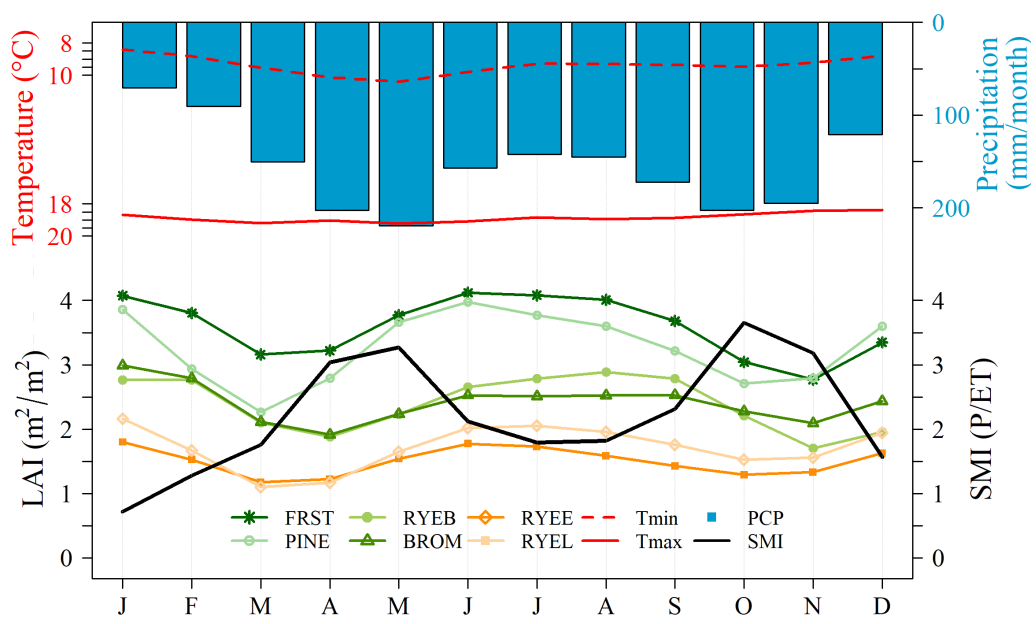


**Figure 2.** Average seasonality of climate variables (1990–2016; gauging stations) and LAI (2003–2016; BFAST-MODIS; area weighted HRU mean) in the CR watershed. Land cover types as in Figure 1.

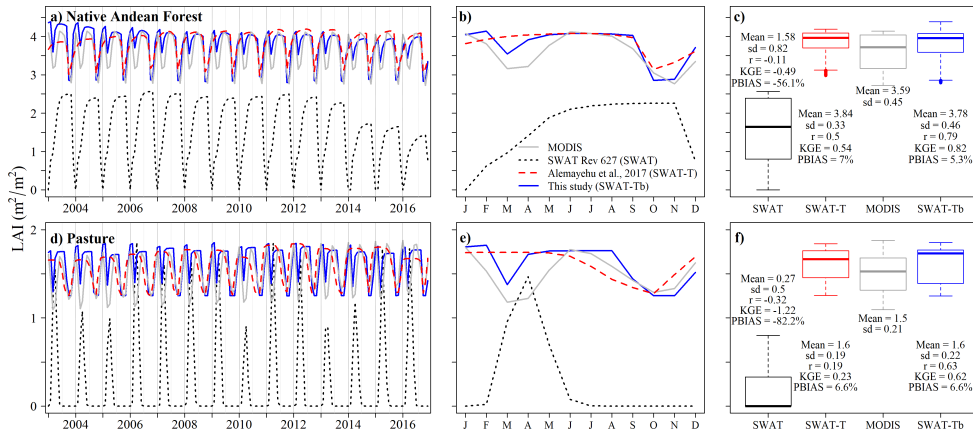


**Figure 3.** Observed (MODIS) and simulated (SWAT, SWAT-T, and SWAT-Tb) seasonality of LAI in the CR watershed for native Andean forest (top) and pasture (bottom). Time series (a, d), average annual cycle (b, e), and the corresponding box-plots and performance statistics (c, f).

assumption of the SWAT model is that LAI is zero at the beginning of each simulation year, which is unrealistic for tropical vegetation. This assumption is kept for the proof-of-concept, and because it is behind an important limitation of SWAT for tropical watersheds (Strauch & Volk, 2013; Mwangi et al., 2016; Alemayehu et al., 2017; Hoyos et al., 2019; H. Zhang et al., 2020). Regardless of whether this assumption is changed, SWAT does not reproduce LAI bimodality. Calibrated SWAT-T realistically reproduces the range of variability of LAI but fails to represent LAI bimodality because it has a prescribed unimodal regime with a single vegetation growth cycle per year (Alemayehu et al., 2017; Hoyos et al., 2019). Calibrated SWAT-Tb outperforms both SWAT and SWAT-T in reproducing the observed bimodality of LAI, as indicated by the correlation values.

#### 4.2 Streamflow Calibration and Validation

SWAT-Tb is calibrated for streamflow by varying the most sensitive parameters (Supplementary Table S3). The best-fit parameter values and acceptable ranges (i.e. range of parameter values for which simulations are acceptably realistic) are presented in Table 2. Simulated and observed monthly streamflow are shown in Figure 4 for the calibration (2003–2016) and validation (1993–2002) periods. Based on multiple criteria (NSE, RSR, and PBIAS), the model performance can be considered as “very good” and “good” for calibration and validation, respectively (Moriasi et al., 2007). Furthermore, water balance components are realistic as compared to the reference values (Supplementary Table S4).

Likewise, using the best-fit parameter values in Table 2, the performance of standard SWAT in reproducing observed streamflow varies between “very good” (for calibration) and “good” (for validation) (Moriasi et al., 2007, Supplementary Figure S2). This illustrates how standard SWAT can show high performance to reproduce streamflow despite having a low capability to simulate dynamics of LAI (Figure 3 and Supplementary Figure S1).

#### 4.3 Forest versus Pasture Impacts on Streamflow

SWAT-Tb results show that the potential impact of forest cover change on the watershed response is much more pronounced in monthly (Figure 5c) than in annual streamflow (Figure 5f). The results based on annual streamflow would misleadingly indicate that there are small differences between the FOR and PAS scenarios. In contrast, forest change leads to

**Table 2.** Best-fit values for parameters and their acceptable range for the calibrated SWAT-Tb model.

Parameter <sup>1</sup>	Description	Scaling type <sup>2</sup>	Range min	Range max	Best-fit value
CN2.mgt_RYEL	Runoff curve number for moisture condition II.	r	-0.22	-0.20	-0.20
ESCO.hru_RYEL	Soil evaporation compensation factor.	v	0.35	0.50	0.42
ESCO.hru_FRST	Soil evaporation compensation factor.	v	0.25	0.40	0.27
ALPHA.BF.gw	Baseflow alpha factor (1/days).	v	0.030	0.045	0.030
CN2.mgt_FRST	Runoff curve number for moisture condition II.	r	-0.20	-0.18	-0.19
SOL.K(1).sol_RYEL	Saturated hydraulic conductivity (mm/hr).	r	-0.35	-0.2	-0.23
GWQMN.gw_FRST	Threshold depth of water in the shallow aquifer required for return flow to occur (mm H <sub>2</sub> O).	v	1500	2000	1988.25
CH_K2.rte	Effective hydraulic conductivity in main channel alluvium (mm/hr).	v	25	75	52.63
GWQMN.gw_RYEL	Threshold depth of water in the shallow aquifer required for return flow to occur (mm H <sub>2</sub> O).	v	2000	2500	2490.25
ESCO.hru_BPWR	Soil evaporation compensation factor.	v	0.15	0.30	0.29
SOL.K(1).sol_FRST	Saturated hydraulic conductivity (mm/hr).	r	-0.20	-0.10	-0.16
SOL.BD(1).sol_BPWR	Moist bulk density (g/cm <sup>3</sup> ).	r	-0.15	0.0	-0.039
CN2.mgt_BPWR	Runoff curve number for moisture condition II.	r	-0.18	-0.15	-0.17
SOL.AWC(1).sol_FRST	Available water capacity of the soil layer (mm H <sub>2</sub> O/mm soil).	r	-0.30	-0.15	-0.25
SOL.BD(1).sol_RYEL	Moist bulk density (g/cm <sup>3</sup> ).	r	0.15	0.25	0.24
GWQMN.gw_BPWR	Threshold depth of water in the shallow aquifer required for return flow to occur (mm H <sub>2</sub> O).	v	1800	2200	1866.20
SOL.K(1).sol_BPWR	Saturated hydraulic conductivity (mm/hr).	r	-0.15	0.0	-0.08
SOL.AWC(1).sol_RYEL	Available water capacity of the soil layer (mm H <sub>2</sub> O/mm soil).	r	0.35	0.50	0.37

<sup>1</sup>Numbers (1, 2) refer to the soil layer number. FRST: native Andean forest, RYEL: pasture, and BPWR: paramo vegetation, planted forest, shrubs, and pasture with secondary growth. <sup>2</sup>Scaling type: v (absolute) indicates that the parameter is replaced by the given value, r (relative) indicates that the parameter is multiplied by [1 + (given value)], which preserves spatial variability.

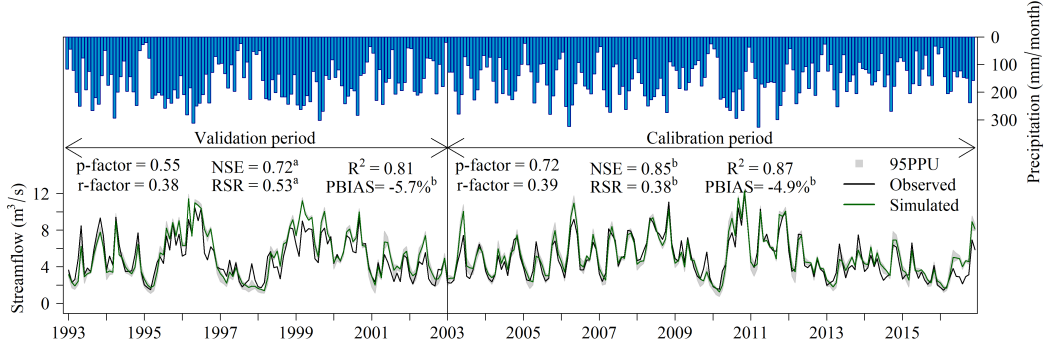


**Figure 4.** Calibration (2003–2016) and validation (1993–2002) of SWAT-Tb for monthly streamflow. Vertical bars show monthly rainfall from SWAT output, calculated from records in climate stations. NSE: Nash-Sutcliffe coefficient, PBIAS: percent bias,  $R^2$ : coefficient of determination, and RSR: RMSE-observations standard deviation ratio. 95PPU: the 95% prediction uncertainty. Model performances based on the criteria of Moriasi et al. (2007): <sup>a</sup> Good ( $0.65 < \text{NSE} \leq 0.75$ ,  $0.50 < \text{RSR} \leq 0.60$ ,  $\pm 10\% < \text{BIAS} < \pm 15\%$ ) and <sup>b</sup> Very Good ( $0.75 < \text{NSE} \leq 1.00$ ,  $0.00 < \text{RSR} \leq 0.50$ ,  $\text{BIAS} \leq \pm 10\%$ ).

330 significant differences in monthly streamflow seasonality, which are particularly pronounced  
 331 during the dry seasons (DJF and JJA). The occurrence of 100% forest cover in the watershed  
 332 leads to increased streamflow during the dry seasons (e.g. average streamflow in January  
 333 is about 10% greater in the FOR than in the CTL scenario), whereas its absence causes  
 334 a streamflow reduction (e.g. average streamflow in January is about 6% lower in the PAS  
 335 than in the CTL scenario). During the wet seasons, the most significant difference is found  
 336 in April when streamflow is reduced in the FOR scenario, while it is increased in the PAS  
 337 scenario. Differences between scenarios are smaller in the SON wet season. These results  
 338 remain valid when considering 1000 combinations of parameters values within the acceptable  
 339 ranges (Supplementary Figure S3).

340 Differences between scenarios seem small when looking at box-plots for the annual cycle  
 341 (Figure 5b) and annual average (Figure 5e). This is because these box-plots do not show  
 342 the year-to-year variability of monthly streamflow. Figures 5c and 5f clarify this by showing  
 343 the distribution (box-plots) of monthly differences computed as the difference of stream-  
 344 flow between scenarios for the same month and year. This is important to guarantee that  
 345 the comparison is done between LULC scenarios under the same climate forcing (precipi-  
 346 tation and temperature). For instance, PAS scenario streamflow under La Niña conditions  
 347 (above-normal precipitation) is not comparable to FOR scenario streamflow under El Niño  
 348 conditions (below-normal precipitation).

349 Despite their comparable ability to reproduce observed streamflow, SWAT and SWAT-  
 350 Tb results do not support the same conclusions. For instance, streamflow increase in the  
 351 FOR scenario during the dry seasons is largely underestimated (in DJF) or even reversed (in  
 352 July and August) (Figure 5c) in SWAT output. The median percent increase of streamflow  
 353 from SWAT can be less than half the corresponding increase in SWAT-Tb (e.g.  $\sim 4\%$  versus  
 354  $\sim 10\%$  in January). Further, SWAT results indicate that the median annual streamflow  
 355 would barely change due to extensive modification of LULC in the FOR and PAS scenarios  
 356 (Figure 5d). In contrast, SWAT-Tb output show a greater change in the median annual  
 357 streamflow. The statistical significance of this change will be discussed below.

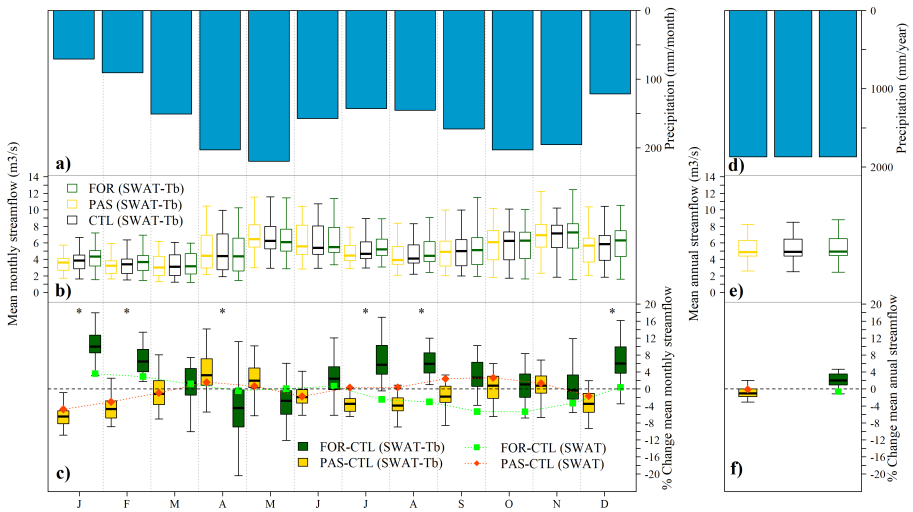


**Figure 5.** Comparison of monthly (left) and annual (right) streamflow between scenarios and models. Input precipitation (blue bars) is the same for all scenarios and models (a,d). Average annual cycle (b) and annual streamflow (e) in all scenarios for 1993–2016. Percent differences between monthly (c) and annual (f) streamflow in the control (CTL) and LULC (FOR and PAS) scenarios for 1993–2016 as simulated by SWAT-Tb and SWAT using best fit parameters. Positive (negative) values indicate that streamflow is increased (decreased) in the LULC change scenario. Boxes (dark green and yellow) show variability of monthly differences in SWAT-Tb output, whereas lines with dots (light green and orange) show the corresponding median from SWAT output. Asterisks identify months for which the difference between medians in the FOR and PAS scenarios is statistically significant ( $n=24$ ,  $p < 0.05$ ) for SWAT-Tb output.

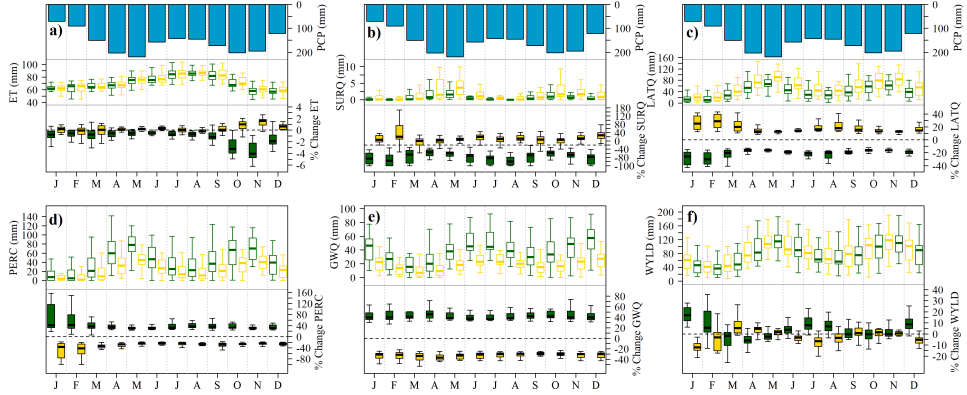


**Figure 6.** Annual cycle and percent differences between monthly (a) actual evapotranspiration (ET), (b) surface runoff (SURQ), (c) lateral flow (LATQ), (d) percolation (PERC), (e) groundwater contribution to streamflow (GWQ), and (f) water yield (WYLD) in the control (CTL) and LULC (FOR and PAS) scenarios for 1993–2016 as simulated by SWAT-Tb at the watershed scale. Variables are HRU area-weighted means for each month. Positive (negative) values indicate that the variable is increased (decreased) in the LULC change scenario. Vertical bars show mean monthly precipitation (PCP).

358

#### 4.4 Water Balance Components

359  
360  
361  
362  
363  
364  
365  
366

Differences in streamflow between scenarios are caused by differences in the watershed's water balance components (Figure 6). The largest differences between the CTL and LULC scenarios are found for surface runoff (Figure 6b), lateral flow (Figure 6c), percolation (Figure 6d), and groundwater contribution (i.e. baseflow) to streamflow (Figure 6e). The sum of these differences leads to differences in water yield (Figure 6f). By comparison, differences in evapotranspiration are much less pronounced (Figure 6a; note that their magnitudes never exceed 6%). All these differences consider the year-to-year variability as explained previously for Figure 5.

367  
368  
369  
370  
371  
372  
373  
374  
375  
376  
377  
378  
379  
380

In our simulations, differences between output from SWAT-Tb and SWAT are entirely caused by differences in the simulated LAI values (Figure 7a). The resulting differences in water balance components are more pronounced for the PAS than for the FOR scenario (Figure 7b–g). As compared to SWAT-Tb, in the PAS scenario SWAT overestimates water yield throughout the year (Figure 7g), with larger values during JJA and SON, i.e. during the second dry and wet seasons of the year in the actual bimodal regime. This overestimation in JJA–SON results from greater production of surface runoff (Figure 7c), lateral flow (Figure 7d), and base flow (Figure 7f), as well as from reduced evapotranspiration (Figure 7b). In DJF–MAM, there are mixed patterns in the water balance components that lead to a smaller overestimation of water yield. In the FOR scenario, SWAT underestimates LAI throughout the year, mostly in DJF, which leads to mixed results in water balance components. In both scenarios, differences of surface runoff between models (Figure 7c) are minimal ( $< \pm 0.5$  mm), hence the effects on streamflow result mainly from variations in evapotranspiration and groundwater flows (i.e. lateral flow, percolation, and base flow).

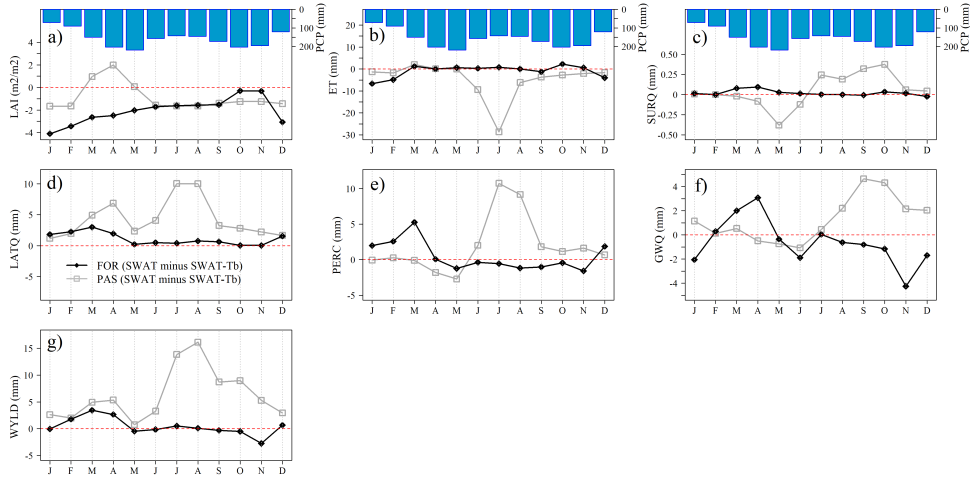


**Figure 7.** Differences between SWAT and SWAT-Tb in the monthly median of (a) Leaf Area Index (LAI), (b) total biomass (BIOM, i.e. above-ground and roots at the end of the period reported as dry weight), (c) actual evapotranspiration (ET), (d) surface runoff (SURQ), (e) lateral flow (LATQ), (f) percolation (PERC), (g) groundwater contribution (GWQ), and (h) water yield (WYLD) for each LULC scenario (PAS and FOR) at the watershed scale (area-weighted HRU mean for each month).

381

## 5 Discussion

382

### 5.1 Advantages of SWAT-Tb over SWAT

383  
384  
385  
386  
387

There is no noticeable difference between SWAT-Tb and SWAT in representing monthly streamflow (Figures 5b and S2). However, there are visible differences in their capability to reproduce vegetation dynamics through LAI (Figure 3), as well as in their results regarding the potential impact of forest conversion on streamflow (Figure 5c) and the underlying changes in the water balance components (Figure 7).

388  
389  
390  
391  
392  
393  
394  
395

Our proof-of-concept illustrates how SWAT can be calibrated to realistically simulate streamflow despite being intrinsically unable to reproduce the observed dynamics of LAI, which has multiple effects on the water balance components including evapotranspiration, canopy interception, and surface runoff (Neitsch et al., 2011; Strauch & Volk, 2013; Alemanyehu et al., 2017). Hence, there is a danger of getting the right results (e.g. the model reproduces observed streamflow) for the wrong reasons (Kirchner, 2006), which strongly limits the capability of models (i.e. SWAT in the present case) to produce reliable results for informing decisions.

396  
397  
398  
399  
400  
401  
402  
403

We argue that SWAT results (Figures 5 and 7), and perhaps also the results of studies using the approach of calibrating and validating SWAT for streamflow but not for LAI (e.g. Villamizar et al., 2019; Adhikari et al., 2020), may be misleading about the impacts of tropical forest change on streamflow. In contrast, SWAT-Tb provides better insight by reproducing not only the observed streamflow but also the bimodal dynamics of LAI that are typical of many tropical watersheds. This is particularly important for assessing water balance components that affect water security in the tropical Andes threatened by undergoing deforestation (A. Salazar et al., 2018; Vivioli et al., 2020).

404           **5.2 Forest Impact on the Watershed's Regulation Capacity and Water Avail-**  
 405           **ability**

406           Results of previous studies about forest change impacts on streamflow are diverse  
 407 (M. Zhang et al., 2017; Ochoa-Tocachi et al., 2016; Jones et al., 2020), which suggests that  
 408 conclusions about this are hardly generalizable. However, a number of previous studies have  
 409 concluded that increased forest cover in a watershed leads to decreased annual streamflow,  
 410 mainly as a consequence of increased evapotranspiration (Ellison et al., 2012; Muñoz-Villers  
 411 & McDonnell, 2013; Ogden et al., 2013; M. Zhang et al., 2017). In our results, differences  
 412 in annual streamflow between scenarios are not statistically significant ( $p > 0.05$ ; Figure 5f  
 413 and Supplementary Figure S3f), which does not necessarily imply that these differences are  
 414 negligible or physically meaningless (Amrhein et al., 2019). Given this, and in addition to  
 415 the significant differences in the annual cycle, our results indicate that annual streamflow is  
 416 almost always greater in the FOR than in the CTL and PAS scenarios, which is opposite to  
 417 the aforementioned conclusion.

418           There are statistically significant differences in monthly streamflow between scenarios  
 419 ( $p < 0.05$ ; Figure 5c and Supplementary Figure S3c), particularly in dry seasons (DJF and  
 420 JJA). This is relevant from the perspective of regulation, defined here as the capacity of  
 421 watersheds to reduce streamflow variability and attenuating extreme streamflows (Ochoa-  
 422 Tocachi et al., 2016; J. F. Salazar et al., 2018; Rodríguez et al., 2018). This regulation  
 423 implies a contrasting capacity of watersheds to increase low streamflows while reducing  
 424 floods (J. F. Salazar et al., 2018; Rodríguez et al., 2018). The CR watershed's regulation  
 425 capacity is increased in the FOR scenario, as revealed by higher streamflow during the dry  
 426 season while little change during the wet season, relative to the CTL scenario.

427           Increased forest cover leads to reduced direct runoff and lateral flow, as well as to  
 428 increased percolation and groundwater contribution to streamflow (i.e. base flow), as com-  
 429 pared to the effect of increased pasture cover (Figure 6), which is consistent with field  
 430 observations in the region of the CR watershed by García-Leoz et al. (2017); Suescún et al.  
 431 (2017). Although these effects of forest change are the same throughout the year (Figure  
 432 6), their impact on streamflow is not the same because it depends on the relative contribu-  
 433 tion of each water balance component to streamflow. In dry seasons, streamflow depends  
 434 more on base flow than on direct runoff and lateral flow. In contrast, during wet seasons  
 435 precipitation may contribute more to streamflow via direct runoff and lateral flow than base  
 436 flow. As a result, the impacts on streamflow of reduced direct runoff and lateral flow, and  
 437 increased percolation and base flow, vary across seasons. The increased presence of forest  
 438 can increase low streamflow during dry seasons mainly through increased base flow, while  
 439 it can reduce streamflow during the wet season mainly through reduced direct runoff and  
 440 lateral flow.

441           These results are consistent with some theoretical hypothesis and previous observational  
 442 studies. The infiltration trade-off hypothesis for tropical environments (Brujinzeel, 1989,  
 443 2004) proposes that reduced forest cover in a watershed can lead to reduced low streamflow  
 444 in dry seasons as a result of reductions in infiltration and water storage in soils during wet  
 445 seasons, which are not compensated by water gains due to reduced evapotranspiration. The  
 446 forest reservoir hypothesis (J. F. Salazar et al., 2018) proposes that tropical forests enhance  
 447 the capacity of watersheds to regulate streamflow, mainly through their role in mediating  
 448 land-atmosphere interactions. Ellison et al. (2012) divide the forest water debate into two  
 449 schools of thought: the “demand-side” and the “supply-side” schools. While the former  
 450 sees trees and forests as consumers of available water and competitors for other downstream  
 451 water uses, the latter supports the beneficial impact of forest cover on the hydrological cycle,  
 452 emphasizing that increasing forest cover raises water yield. Our results lend support to the  
 453 “supply-side” perspective.

454           Observational and modeling studies have shown that forest conversion into pasture or  
 455 croplands in tropical watersheds can result in decreased low streamflows and increased floods

(Roa-García et al., 2011; Ogden et al., 2013; Ochoa-Tocachi et al., 2016; Ramírez et al., 2017; Krishnaswamy et al., 2018; Peña-Arancibia et al., 2019; López-Ramírez et al., 2020). Our results indicate that forest cover gain (i.e. FOR scenario) leads to increased infiltration and groundwater recharge (Figures 6c-e) and little changes in evapotranspiration (Figures 6a). Field observations in the region of the CR watershed have indicated that the difference between evapotranspiration of native Andean forest (FRST) and pasture (RYEL) is small (García-Leoz et al., 2017), as it is in our results.

## 463 6 Conclusions

464 Bimodal seasonal patterns of vegetation dynamics are common to many watersheds,  
 465 especially (although not exclusively) in tropical regions under the influence of the ITCZ.  
 466 The new SWAT-Tb variant reproduces not only observed streamflow, but also the bimodal  
 467 seasonal pattern of LAI in a tropical mountain watershed. In contrast, standard SWAT  
 468 is inherently unable to reproduce this bimodality in vegetation dynamics, although it can  
 469 be calibrated to reproduce streamflow. These variations in the representation of LAI sea-  
 470 sonality can lead to significantly different results when assessing LULC change impacts on  
 471 streamflow.

472 Regarding the effect of forest change on streamflow, our results show that impacts  
 473 can be much more pronounced for seasonal than for annual streamflow, and indicate that  
 474 forests can play a crucial role in enhancing water availability during dry seasons. We found  
 475 that the seasonality of streamflow anomalies is largely switched due to forest-to-pasture  
 476 conversion, implying that while forest expansion increases water availability in dry seasons,  
 477 deforestation (e.g. forest conversion into pasture) can strongly decrease it. Due to its poor  
 478 representation of LAI seasonality, standard SWAT largely underestimates this role of forest,  
 479 which can be misleading for decision making about water security and forest conservation.

## 480 Data availability

481 The SWAT-Tb executable and code will be available through SWATshare ([https://mygeohub.org/groups/water-hub/swatshare\\_landing](https://mygeohub.org/groups/water-hub/swatshare_landing)), which is a cyberinfrastructure for  
 482 sharing, simulation, and visualization of SWAT models. For review purposes, the data  
 483 are available online at <https://bit.ly/2XT8uxs>. After publication, we may change the  
 484 link to keep the files permanently available in SWATshare. Emails requesting necessary  
 485 technical support can be directed to the corresponding author. The data used in this  
 486 study are publicly available. Sources to access these data, including any other information  
 487 to replicate the results, are provided in the references, tables, and supporting  
 488 information. Also, they are accessible through links provided below: Digital Elevation  
 489 Model was from <http://srtm.csi.cgiar.org/>. MODIS-LAI data was obtained from  
 490 <https://lpdaac.usgs.gov/products/mcd15a2hv006/>. IDEAM from  
 491 <http://dhime.ideam.gov.co/atencionciudadano/>. Land cover and soil types maps is  
 492 available through CORANTIOQUIA and UNAL (2015) and Machado et al. (2019), respec-  
 493 tively.

## 495 Acknowledgments

496 This work was funded by the Universidad de Antioquia through the Estudiante Instructor  
 497 Program for graduate studies and Committee for Research Development. JFS and  
 498 JCV were funded by the Colombian Ministry of Science, Technology and Innovation (MIN-  
 499 CIENCIAS) through program “Sostenibilidad de sistemas ecológicos y sociales en la cuenca  
 500 Magdalena-Cauca bajo escenarios de cambio climático y pérdida de bosques” (code 1115-  
 501 852-70719) with funds from “Patrimonio Autónomo Fondo Nacional de Financiamiento para  
 502 la Ciencia, la Tecnología y la Innovación, Fondo Francisco José de Caldas”. JCV was sup-  
 503 ported by the project “Trayectorias de sistemas socio-ecológicos y sus determinantes en

504 cuencas estratégicas en un contexto de cambio ambiental. Código 110180863961, Convocatoria 505 808-2018 Proyectos de ciencia, tecnología e innovación y su contribución a los retos de 506 país-Colciencias". NH was partially supported by the Fulbright Visiting Scholar Program 507 from the Fulbright Commission in Colombia while on research leave from Universidad del 508 Norte, and by The Canadian Queen Elizabeth II Diamond Jubilee Scholarships (QES), a 509 partnership among Universities in Canada, the Rideau Hall Foundation (RHF), Community 510 Foundations of Canada (CFC). The QES-AS is made possible with financial support from 511 IDRC and SSHRC. The authors are grateful to Natalia Uribe and Jenny Machado for their 512 support with setting up SWAT.

## 513 References

- 514 Abbaspour, K. C. (2013). SWAT-CUP 2012. *SWAT Calibration and Uncertainty Pro-*  
 515 *gram—A User Manual.*
- 516 Abbaspour, K. C., Johnson, C., & Van Genuchten, M. T. (2004). Estimating uncertain flow  
 517 and transport parameters using a sequential uncertainty fitting procedure. *Vadose*  
 518 *Zone Journal*, 3(4), 1340–1352.
- 519 Abbaspour, K. C., Rouholahnejad, E., Vaghefi, S., Srinivasan, R., Yang, H., & Kløve, B.  
 520 (2015). A continental-scale hydrology and water quality model for Europe: Calibration  
 521 and uncertainty of a high-resolution large-scale SWAT model. *Journal of Hydrology*,  
 522 524, 733–752.
- 523 Adhikari, R. K., Mohanasundaram, S., & Shrestha, S. (2020). Impacts of land-use changes on  
 524 the groundwater recharge in the Ho Chi Minh city, Vietnam. *Environmental Research*,  
 525 109440.
- 526 Alemayehu, T., Griensven, A. v., Woldegiorgis, B. T., & Bauwens, W. (2017). An improved  
 527 SWAT vegetation growth module and its evaluation for four tropical ecosystems. *Hydrology*  
 528 and Earth System Sciences
- 529 Alhamad, M., Stuth, J., & Vannucci, M. (2007). Biophysical modelling and NDVI time  
 530 series to project near-term forage supply: spectral analysis aided by wavelet denoising  
 531 and ARIMA modelling. *International Journal of Remote Sensing*, 28(11), 2513–2548.
- 532 Alvarenga, L., De Mello, C., Colombo, A., Cuartas, L., & Bowling, L. (2016). Assessment  
 533 of land cover change on the hydrology of a Brazilian headwater watershed using the  
 534 Distributed Hydrology-Soil-Vegetation Model. *Catena*, 143, 7–17.
- 535 Amrhein, V., Greenland, S., & McShane, B. (2019). *Scientists rise up against statistical*  
 536 *significance*. Nature Publishing Group.
- 537 Angarita, H., Wickel, A. J., Sieber, J., Chavarro, J., Maldonado-Ocampo, J. A., Herrera-R,  
 538 G. A., ... Purkey, D. (2018). Basin-scale impacts of hydropower development on  
 539 the Mompós Depression wetlands, Colombia. *Hydrology and Earth System Sciences*,  
 540 22(5), 2839.
- 541 Aparecido, L. M. T., Teodoro, G. S., Mosquera, G., Brum, M., Barros, F. d. V., Pompeu,  
 542 P. V., ... others (2018). Ecohydrological drivers of Neotropical vegetation in montane  
 543 ecosystems. *Ecohydrology*, 11(3), e1932.
- 544 Arnold, J., Moriasi, D. N., Gassman, P. W., Abbaspour, K. C., White, M. J., Srinivasan,  
 545 R., ... others (2012). Swat: Model use, calibration, and validation. *Transactions of*  
 546 *the ASABE*, 55(4), 1491–1508.
- 547 Arnold, J., Srinivasan, R., Muttiah, R. S., & Williams, J. R. (1998). Large area hydrologic  
 548 modeling and assessment part I: model development. *JAWRA Journal of the American*  
 549 *Water Resources Association*, 34(1), 73–89.
- 550 Bauer, D. F. (1972). Constructing confidence sets using rank statistics. *Journal of the*  
 551 *American Statistical Association*, 67(339), 687–690.
- 552 Benavides, I., Solarte, M., Pabón, V., Ordoñez, A., Beltrán, E., Rosero, S., & Torres, C.  
 553 (2018). The variation of infiltration rates and physical-chemical soil properties across  
 554 a land cover and land use gradient in a Paramo of southwestern Colombia. *Journal of*  
 555 *Soil and Water Conservation*, 73(4), 400–410.
- 556 Berrouet, L., Villegas-Palacio, C., & Botero, V. (2020). Vulnerability of Rural Communities

- 557 to Change in an Ecosystem Service Provision: Surface water supply. A Case Study in  
 558 the Northern Andes, Colombia. *Land Use Policy*, 97, 104737.
- 559 Bonan, G. B. (2008). Forests and climate change: forcings, feedbacks, and the climate  
 560 benefits of forests. *science*, 320(5882), 1444–1449.
- 561 Bonnesoeur, V., Locatelli, B., Guariguata, M. R., Ochoa-Tocachi, B. F., Vanacker, V., Mao,  
 562 Z., ... Mathez-Stiefel, S.-L. (2019). Impacts of forests and forestation on hydrological  
 563 services in the Andes: A systematic review. *Forest Ecology and Management*, 433,  
 564 569–584.
- 565 Bruijnzeel, L. (1989). forestation and dry season flow in the tropics: A closer look. *Journal*  
 566 of *Tropical Forest Science*, 229–243.
- 567 Bruijnzeel, L. (2004). Hydrological functions of tropical forests: not seeing the soil for the  
 568 trees? *Agriculture, ecosystems & environment*, 104(1), 185–228.
- 569 Clerici, N., Cote-Navarro, F., Escobedo, F. J., Rubiano, K., & Villegas, J. C. (2019).  
 570 Spatio-temporal and cumulative effects of land use-land cover and climate change on  
 571 two ecosystem services in the Colombian Andes. *Science of The Total Environment*,  
 572 685, 1181–1192.
- 573 CORANTIOQUIA, & UNAL. (2015). *Actualización y ajuste plan de ordenación y manejo de*  
 574 *la cuenca de los ríos grande y chico. municipios de belmira, san pedro de los milagros,*  
 575 *entrerríos, santa rosa de osos, donmatías y yarumal. (no. convenio interadministrativo*  
 576 *no. 967 de 2013)* (Tech. Rep.). Medellín, Antioquia: Corporación Autónoma Regional  
 577 del Centro de Antioquia y Universidad Nacional de Colombia Sede Medellín.
- 578 Dile, Y., Srinivasan, R., & George, C. (2019). QGIS Interface for SWAT (QSWAT), version  
 579 1.9. *Texas AM University*.
- 580 Dos Santos, V., Laurent, F., Abe, C., & Messner, F. (2018). Hydrologic Response to Land  
 581 Use Change in a Large Basin in Eastern Amazon. *Water*, 10(4), 429.
- 582 Duque-Villegas, M., Salazar, J. F., & Rendón, A. M. (2019). Tipping the ENSO into a  
 583 permanent El Niño can trigger state transitions in global terrestrial ecosystems. *Earth*  
 584 *System Dynamics*, 10(4).
- 585 Ellison, D., N. Futter, M., & Bishop, K. (2012). On the forest cover–water yield debate:  
 586 from demand-to supply-side thinking. *Global Change Biology*, 18(3), 806–820.
- 587 Espinoza, J. C., Garreaud, R., Poveda, G., Arias, P. A., Molina-Carpio, J., Masiokas, M., ...  
 588 Scaff, L. (2020). Hydroclimate of the Andes Part I: Main climatic features. *Frontiers*  
 589 in *Earth Science*, 8, 64.
- 590 Foley, J. A., DeFries, R., Asner, G. P., Barford, C., Bonan, G., Carpenter, S. R., ... others  
 591 (2005). Global consequences of land use. *science*, 309(5734), 570–574.
- 592 García-Leoz, V., Villegas, J. C., Suescún, D., Flórez, C. P., Merino-Martín, L., Betancur,  
 593 T., & León, J. D. (2017). Land cover effects on water balance partitioning in the  
 594 Colombian Andes: improved water availability in early stages of natural vegetation  
 595 recovery. *Regional Environmental Change*, 1–13.
- 596 Gassman, P. W., Sadeghi, A. M., & Srinivasan, R. (2014). Applications of the SWAT model  
 597 special section: overview and insights. *Journal of Environmental Quality*, 43(1), 1–8.
- 598 Gotsch, S. G., Asbjornsen, H., & Goldsmith, G. R. (2016). Plant carbon and water fluxes  
 599 in tropical montane cloud forests. *Journal of Tropical Ecology*, 32(5), 404–420.
- 600 Gupta, H. V., Kling, H., Yilmaz, K. K., & Martinez, G. F. (2009). Decomposition of  
 601 the mean squared error and NSE performance criteria: Implications for improving  
 602 hydrological modelling. *Journal of hydrology*, 377(1-2), 80–91.
- 603 Hasan, M. M., & Wyseure, G. (2018). Impact of climate change on hydropower generation  
 604 in Rio Jubones Basin, Ecuador. *Water Science and Engineering*, 11(2), 157–166.
- 605 Hoyos, N., Correa-Metrio, A., Jepsen, S. M., Wemple, B., Valencia, S., Marsik, M., ...  
 606 Velez, M. I. (2019). Modeling Streamflow Response to Persistent Drought in a Coastal  
 607 Tropical Mountainous Watershed, Sierra Nevada De Santa Marta, Colombia. *Water*,  
 608 11(1), 94.
- 609 Immerzeel, W. W., Lutz, A., Andrade, M., Bahl, A., Biemans, H., Bolch, T., ... others  
 610 (2020). Importance and vulnerability of the world's water towers. *Nature*, 577(7790),  
 611 364–369.

- 612 Jaramillo-Robledo, A. (2003). La lluvia y el transporte de nutrientos dentro de ecosistemas  
613 de bosque y cafetales. *Cenicafé*, 54(2), 134–144.
- 614 Jarvis, A., Reuter, H. I., Nelson, A., Guevara, E., et al. (2008). Hole-filled SRTM for the  
615 globe Version 4. available from the CGIAR-CSI SRTM 90m Database ([http://srtm.cgiar.org](http://srtm.csi.cgiar.org)), 15, 25–54.
- 616 Jones, J. A., Wei, X., Archer, E., Bishop, K., Blanco, J. A., Ellison, D., ... Creed, I. F.  
617 (2020). Forest-water interactions under global change. In *Forest-Water Interactions*  
618 (pp. 589–624). Springer.
- 619 Kirchner, J. W. (2006). Getting the right answers for the right reasons: Linking measurements,  
620 analyses, and models to advance the science of hydrology. *Water Resources Research*, 42(3).
- 621 Knoben, W. J., Woods, R. A., & Freer, J. E. (2019). Global bimodal precipitation seasonality:  
622 A systematic overview. *International Journal of Climatology*, 39(1), 558–567.
- 623 Krishnaswamy, J., Kelkar, N., & Birkel, C. (2018). Positive and neutral effects of forest cover  
624 on dry-season stream flow in Costa Rica identified from Bayesian regression models  
625 with informative prior distributions. *Hydrological Processes*, 32(24), 3604–3614.
- 626 Krysanova, V., Vetter, T., Eisner, S., Huang, S., Pechlivanidis, I., Strauch, M., ... others  
627 (2017). Intercomparison of regional-scale hydrological models and climate change  
628 impacts projected for 12 large river basins worldwide—a synthesis. *Environmental  
Research Letters*, 12(10), 105002.
- 629 Li, F., Zhang, G., Li, H., & Lu, W. (2019). Land Use Change Impacts on Hydrology in the  
630 Nenjiang River Basin, Northeast China. *Forests*, 10(6), 476.
- 631 Liang, B., Chen, X., Lang, W., Liu, G., Malhi, Y., & Rifai, S. (2020). Examining land  
632 surface phenology in the tropical moist forest eco-zone of South America. *International  
Journal of Biometeorology*, 1–12.
- 633 López-Ramírez, S. M., Sáenz, L., Mayer, A., Muñoz-Villers, L. E., Asbjornsen, H., Berry,  
634 Z. C., ... Aguilar, L. R. G. (2020). Land use change effects on catchment streamflow  
635 response in a humid tropical montane cloud forest region, central veracruz, mexico.  
636 *Hydrological Processes*.
- 637 Ma, T., Duan, Z., Li, R., & Song, X. (2019). Enhancing SWAT with remotely sensed LAI  
638 for improved modelling of ecohydrological process in subtropics. *Journal of hydrology*,  
639 570, 802–815.
- 640 Machado, J., Villegas-Palacio, C., Loaiza, J. C., & Castañeda, D. A. (2019). Soil natural  
641 capital vulnerability to environmental change. A regional scale approach for tropical  
642 soils in the Colombian Andes. *Ecological indicators*, 96, 116–126.
- 643 Marín, F., Dahik, C. Q., Mosquera, G. M., Feyen, J., Cisneros, P., & Crespo, P. (2019).  
644 Changes in soil hydro-physical properties and SOM due to Pine afforestation and  
645 grazing in Andean environments cannot be generalized. *Forests*, 10(1), 17.
- 646 Marin, M., Clinciu, I., Tudose, N. C., Ungurean, C., Adorjani, A., Mihalache, A. L., ...  
647 Cacovean, H. (2020). Assessing the vulnerability of water resources in the context of  
648 climate changes in a small forested watershed using SWAT: A review. *Environmental  
Research*, 109330.
- 649 Mercado-Bettín, D., Salazar, J. F., & Villegas, J. C. (2019). Long-term water balance  
650 partitioning explained by physical and ecological characteristics in world river basins.  
651 *Ecohydrology*, 12(3), e2072.
- 652 Montanari, A., Young, G., Savenije, H., Hughes, D., Wagener, T., Ren, L., ... Belyaev, V.  
653 (2013). “Panta Rhei—everything flows”: change in hydrology and society—the IAHS  
654 scientific decade 2013–2022. *Hydrological Sciences Journal*, 58(6), 1256–1275.
- 655 Moriasi, D. N., Arnold, J., Van Liew, M. W., Bingner, R. L., Harmel, R. D., & Veith,  
656 T. L. (2007). Model evaluation guidelines for systematic quantification of accuracy in  
657 watershed simulations. *Transactions of the ASABE*, 50(3), 885–900.
- 658 Muñoz-Villers, L., & McDonnell, J. (2013). Land use change effects on runoff generation in  
659 a humid tropical montane cloud forest region. *Hydrology and Earth System Sciences*,  
660 17(9), 3543.
- 661 Mwangi, H. M., Julich, S., Patil, S. D., McDonald, M. A., & Feger, K.-H. (2016). Mod-

- 667       elling the impact of agroforestry on hydrology of Mara River Basin in East Africa.  
 668       *Hydrological Processes*, 30(18), 3139–3155.
- 669       Myneni, R., Knyazikhin, Y., & Park, T. (2015). *MCD15A2H MODIS/Terra+ Aqua Leaf*  
 670       *Area Index/FPAR 8-day L4 Global 500 m SIN Grid V006, NASA EOSDIS Land*  
 671       *Processes DAAC*.
- 672       Neitsch, S. L., Arnold, J., Kiniry, J. R., & Williams, J. R. (2011). *Soil and water assessment*  
 673       *tool theoretical documentation version 2009* (Tech. Rep.). College Station, Texas:  
 674       Texas Water Resources Institute.
- 675       Ochoa-Tocachi, B. F., Buytaert, W., De Bievre, B., Céller, R., Crespo, P., Villacís, M., ...  
 676       others (2016). Impacts of land use on the hydrological response of tropical Andean  
 677       catchments. *Hydrological Processes*, 30(22), 4074–4089.
- 678       Ogden, F. L., Crouch, T. D., Stallard, R. F., & Hall, J. S. (2013). Effect of land cover and  
 679       use on dry season river runoff, runoff efficiency, and peak storm runoff in the seasonal  
 680       tropics of central panama. *Water Resources Research*, 49(12), 8443–8462.
- 681       Peña-Arancibia, J. L., Bruijnzeel, L. A., Mulligan, M., & van Dijk, A. I. (2019). Forests  
 682       as ‘sponges’ and ‘pumps’: Assessing the impact of deforestation on dry-season flows  
 683       across the tropics. *Journal of Hydrology*, 574, 946–963.
- 684       Ponette-González, A. G., Marín-Spiotta, E., Brauman, K. A., Farley, K. A., Weathers,  
 685       K. C., & Young, K. R. (2014). Hydrologic connectivity in the high-elevation tropics:  
 686       Heterogeneous responses to land change. *BioScience*, 64(2), 92–104.
- 687       Posada-Marín, J. A., Rendón, A. M., Salazar, J. F., Mejía, J. F., & Villegas, J. C. (2019).  
 688       WRF downscaling improves ERA-Interim representation of precipitation around a  
 689       tropical Andean valley during El Niño: implications for GCM-scale simulation of  
 690       precipitation over complex terrain. *Climate Dynamics*, 52(5-6), 3609–3629.
- 691       Poveda, G. (2004). La hidroclimatología de Colombia: una síntesis desde la escala inter-  
 692       decadal hasta la escala diurna. *Revista de la Academia Colombiana de Ciencias exac-  
 693       tas, físicas y naturales*, 28(107), 201–222.
- 694       Rajib, A., Kim, I. L., Golden, H. E., Lane, C. R., Kumar, S. V., Yu, Z., & Jeyalakshmi,  
 695       S. (2020). Watershed Modeling with Remotely Sensed Big Data: MODIS Leaf Area  
 696       Index Improves Hydrology and Water Quality Predictions. *Remote Sensing*, 12(13),  
 697       2148.
- 698       Ramírez, B. H., Teuling, A. J., Ganzeveld, L., Hegger, Z., & Leemans, R. (2017). Trop-  
 699       ical Montane Cloud Forests: Hydrometeorological variability in three neighbouring  
 700       catchments with different forest cover. *Journal of hydrology*, 552, 151–167.
- 701       Roa-García, M., Brown, S., Schreier, H., & Lavkulich, L. (2011). The role of land use and  
 702       soils in regulating water flow in small headwater catchments of the Andes. *Water*  
 703       *Resources Research*, 47(5).
- 704       Rodríguez, E., Salazar, J. F., Villegas, J. C., & Mercado-Bettín, D. (2018). Assessing  
 705       changes in extreme river flow regulation from non-stationarity in hydrological scaling  
 706       laws. *Journal of Hydrology*, 562, 492–501.
- 707       Sáenz, L., Mulligan, M., Arjona, F., & Gutierrez, T. (2014). The role of cloud forest  
 708       restoration on energy security. *Ecosystem Services*, 9, 180–190.
- 709       Salazar, A., Sanchez, A., Villegas, J. C., Salazar, J. F., Ruiz Carrascal, D., Sitch, S.,  
 710       ... others (2018). The ecology of peace: preparing Colombia for new political and  
 711       planetary climates. *Frontiers in Ecology and the Environment*, 16(9), 525–531.
- 712       Salazar, J. F., Villegas, J. C., Rendón, A. M., Rodríguez, E., et al. (2018). Scaling properties  
 713       reveal regulation of river flows in the Amazon through a “forest reservoir”. *Hydrology*  
 714       *and Earth System Sciences*, 22(3), 1735–1748.
- 715       Setegn, S. G., Srinivasan, R., Melesse, A. M., & Dargahi, B. (2010). Swat model application  
 716       and prediction uncertainty analysis in the lake tana basin, ethiopia. *Hydrological*  
 717       *Processes: An International Journal*, 24(3), 357–367.
- 718       Strauch, M., & Volk, M. (2013). SWAT plant growth modification for improved modeling  
 719       of perennial vegetation in the tropics. *Ecological Modelling*, 269, 98–112.
- 720       Suescún, D., Villegas, J. C., León, J. D., Flórez, C. P., García-Leoz, V., & Correa-Londono,  
 721       G. A. (2017). Vegetation cover and rainfall seasonality impact nutrient loss via runoff

- 722 and erosion in the Colombian Andes. *Regional environmental change*, 17(3), 827–839.
- 723 Tan, M. L., Gassman, P., Yang, X., & Haywood, J. (2020). A Review of SWAT Applications,  
724 Performance and Future Needs for Simulation of Hydro-Climatic Extremes. *Advances  
725 in Water Resources*, 103662.
- 726 Tapasco, J., Quintero, M., Uribe, N., Valencia, J., Calderón, S., Romero, G., ... Ludeña,  
727 C. E. (2015). *Impactos económicos del cambio climático en Colombia: recurso hídrico*  
728 (Tech. Rep.). Washington, D.C.: Banco Interamericano de Desarrollo. Monografía No.  
729 257.
- 730 Tian, F., Lü, Y. H., Fu, B. J., Zhang, L., Zang, C. F., Yang, Y. H., & Qiu, G. Y. (2017).  
731 Challenge of vegetation greening on water resources sustainability: Insights from a  
732 modeling-based analysis in Northwest China. *Hydrological processes*, 31(7), 1469–  
733 1478.
- 734 Tobón, C., Bruijnzeel, L., Frumau, K. A., & Calvo-Alvarado, J. (2010). Changes in soil  
735 physical properties after conversion of tropical montane cloud forest to pasture in  
736 northern Costa Rica. *Tropical montane cloud forests: Science for conservation and  
737 management*, 502–515.
- 738 Uribe, N., Corzo, G., Quintero, M., van Griensven, A., & Solomatine, D. (2018). Impact of  
739 conservation tillage on nitrogen and phosphorus runoff losses in a potato crop system  
740 in Fuquene watershed, Colombia. *Agricultural Water Management*, 209, 62–72.
- 741 Uribe, N., Srinivasan, R., Corzo, G., Arango, D., & Solomatine, D. (2020). Spatio-temporal  
742 critical source area patterns of runoff pollution from agricultural practices in the  
743 Colombian Andes. *Ecological Engineering*, 149, 105810.
- 744 Urrea, V., Ochoa, A., & Mesa, O. (2019). Seasonality of Rainfall in Colombia. *Water  
745 Resources Research*, 55(5), 4149–4162.
- 746 Verbesselt, J., Hyndman, R., Newham, G., & Culvenor, D. (2010). Detecting trend  
747 and seasonal changes in satellite image time series. *Remote sensing of Environment*,  
748 114(1), 106–115.
- 749 Villamizar, S. R., Pineda, S. M., & Carrillo, G. A. (2019). The Effects of Land Use and  
750 Climate Change on the Water Yield of a Watershed in Colombia. *Water*, 11(2), 285.
- 751 Vivioli, D., Dürr, H. H., Messerli, B., Meybeck, M., & Weingartner, R. (2007). Mountains  
752 of the world, water towers for humanity: Typology, mapping, and global significance.  
753 *Water resources research*, 43(7).
- 754 Vivioli, D., Kummu, M., Meybeck, M., Kallio, M., & Wada, Y. (2020). Increasing de-  
755 pendence of lowland populations on mountain water resources. *Nature Sustainability*,  
756 1–12.
- 757 Wagner, P., Kumar, S., Fiener, P., & Schneider, K. (2011). Hydrological modeling with  
758 SWAT in a monsoon-driven environment: experience from the Western Ghats, India.  
759 *Transactions of the ASABE*, 54(5), 1783–1790.
- 760 Williams, J., Jones, C., Kiniry, J., & Spanel, D. A. (1989). The EPIC crop growth model.  
761 *Transactions of the ASAE*, 32(2), 497–0511.
- 762 Yang, W., Long, D., & Bai, P. (2019). Impacts of future land cover and climate changes on  
763 runoff in the mostly afforested river basin in north China. *Journal of hydrology*, 570,  
764 201–219.
- 765 Ye, W., van Dijk, A. I., Huete, A., & Yebra, M. (2021). Global trends in vegetation  
766 seasonality in the gimms ndvi3g and their robustness. *International Journal of Applied  
767 Earth Observation and Geoinformation*, 94, 102238.
- 768 Zemp, D. C., Schleussner, C.-F., Barbosa, H. M., Hirota, M., Montade, V., Sampaio, G., ...  
769 Rammig, A. (2017). Self-amplified Amazon forest loss due to vegetation-atmosphere  
770 feedbacks. *Nature communications*, 8(1), 1–10.
- 771 Zhang, H., Wang, B., Li Liu, D., Zhang, M., Leslie, L. M., & Yu, Q. (2020). Using an  
772 improved SWAT model to simulate hydrological responses to land use change: a case  
773 study of a catchment in tropical Australia. *Journal of Hydrology*, 124822.
- 774 Zhang, M., Liu, N., Harper, R., Li, Q., Liu, K., Wei, X., ... Liu, S. (2017). A global review  
775 on hydrological responses to forest change across multiple spatial scales: Importance  
776 of scale, climate, forest type and hydrological regime. *Journal of Hydrology*, 546,

777

44–59.

778

- Zhang, X., Friedl, M. A., & Schaaf, C. B. (2006). Global vegetation phenology from moderate resolution imaging spectroradiometer (modis): Evaluation of global patterns and comparison with in situ measurements. *Journal of Geophysical Research: Biogeosciences*, 111(G4).

779

780

781